Variable Star and Exoplanet Section of Czech Astronomical Society and Masaryk University

Proceedings of the
49th Conference on Variable Stars Research

Masaryk University (Department of Theoretical Physics and Astrophysics), Brno, Czech Republic, EU

3rd – 5th November 2017

Editor-in-chief   **Radek Kocián**

Participants of the conference

TABLE OF CONTENTS

INTRODUCTION

The Variable Star and Exoplanet Section of the Czech Astronomical Society organized traditional autumn conference on research and news in the field of variable stars. This year the conference was held at Masaryk University in Brno. In addition to many contributions that were presented on site, we had an opportunity to hear lectures given by invited speakers from abroad via Internet. All presented contributions can be viewed on our YouTube channel.

I would like to thank all conference participant and all speakers for their contributions. I also would like to thank the Director of Department of Theoretical Physics and Astrophysics of Masaryk University, prof. Rikard von Unge, Ph.D. for providing venues for conference and to all his colleagues from Department (especially our members prof. RNDr. Zdeněk Mikulášek, CSc. and Assoc.Prof. RNDr. Miloslav Zejda, Ph.D.).

Ladislav Šmelcer

president of Variable Star and Exoplanet

Section of Czech Astronomical Society

Valašské Meziříčí, March 2018

NOTES

The scientific content of the proceedings contributions was not reviewed by the OEJV editorial board.

The variables V477 Peg and MW Com observation results

V. Bahýl[1], M. Gajtanska[2], P. Hanisko[1], Ľ. Krišták[2]

(1)   Júlia Observatory, Zvolenská Slatina, Slovak Republic, basoft@zv.psg.sk

(2)   KFEAM, DF TU Zvolen, Masarykova 24, 960 53 Zvolen, Slovak Republic

Abstract: The paper deals with our results of the photometric observations of two variable stars and with basic interprettions of our results. We have observed the V477 Pegassi and MW Comae systems. We have obtained their light curves in the integral light and in the B, V, R and I filters. The color indices have been computed and there have been realized the models of the both systems by the usage of the BM3 software. These models are presented in our study too.

Introduction

Today, there exist the fully automated sky surveys for the study of the variable stars and according to our opinion there is coming the day, in which, even if not all the stars, but at least most of them will be declared as variables. But one thing is to detect that a certain star is variable but quite other problem is to determine or to study the full character of the variability of such a star. In this fact we allow us to see the space for the individual observations of the variables. More, the astronomy is wonderful science. At least because in the time of the observations the observer had the stars over his head and everyone is such able in the Immanuel Kant´s sense taste the beauty of the heavens. This is according to our opinion not possible through the automated surveys. This is why we decided to observe the individual stars only. In this time we have selected for us relatively neglected objects and from the internet pages of the http://var2.astro.cz/. We have selected the objects V477 Pegasi and MW Comae. Both this objects have the value of the so called "kanadské bodování ~ Canadian score" equal to ten. This means that in the last ten years there has been realized one observation of the system only.

Even if we enter the AAVSO internet pages, this is not as true as it seems at the first sight but so or so these objects are not in the front of the interest of the variable stars observers. We have selected the mentioned objects owing to the up mentioned facts and owing to the limits of our technical possibilities.

Upon the AAVSO internet pages we have found the basic information concerning the both systems. These data we have accepted as the basic ones and we have started our observations.

Observations and analysis

The variables V 477 Peg and MW Com are not frequently observed systems. So, let us introduce them.

The V477 Peg has the coordinates as follow α = 21:55:1.2, δ = +20:20:26. The catalogue number is TYC1687 1479 and V magnitude is 12.266. The variability is of the Beta Lyrae type.

The variable MW Com has the coordinates as follow α = 12:19:11.6, δ = +29:12:01. The catalogue number is TYC 1991 133 and V magnitude is 10.123. The variability is of the Algol type.

V477 Peg

The variable V477 Peg is short period variable with the period P = 0.274751 days. So, there is easy to obtain the complete light curve in a few nights. We have observed this system in the year 2017 in the eight nights as there is given in the subsequent Table 1.

Table 1: Observation nights of V477 Peg

Month	Day	From	To	No. of fits files
July	21.	20:40	24:00	73
	22.	00:00	00:37	14
	29.	20:10	24:00	83
	30.	00:00	00:09	7
August	02.	19:42	24:00	96
	03.	00:00	00:28	14
	13.	22:22	22:59	29
	15.	19:25	21:01	92

In common, we have obtained 2040 fits files of the observations of this system. The weather conditions have been well and the sky had been clear. The selection of the comparison (TYC 1687 1482) and of the check (3UC221-297463) star is on the Figure 1.
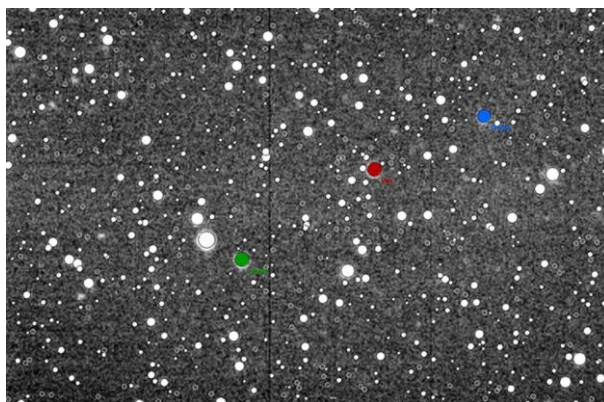

Figure 1: The selection of the comparison star and of the check star for the V477 Peg variable

We have obtained complete light curves in the filters B, V, R and I through the course of our observations. Moreover, we have obtained the complete light curve in the integral light too as we have one window of our filter wheel empty.

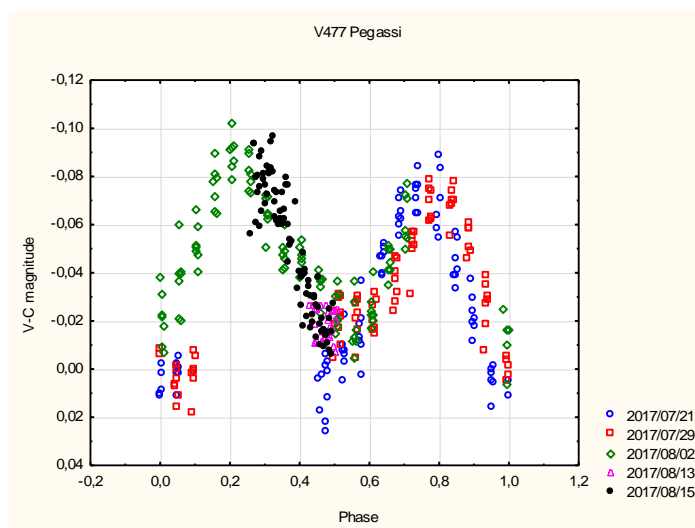The basic light curve composed from all our observations for the integral light is on the Figure 2.

Figure 2: The common light curve

MW Com

The variable MW Comae is typical Algol type variable. Its period is P = 2.1677 days. So it is rather difficult to be observed in our conditions but our observational effort allows us to construct the whole light curve from our observations. We have observed this system in the thirty nights according to the table 2. The weather conditions have been well and the sky had been clear. The exposure time was 30 seconds. The amount of the fits files is the same for all the filters so in common we have obtained 7935 files at all.
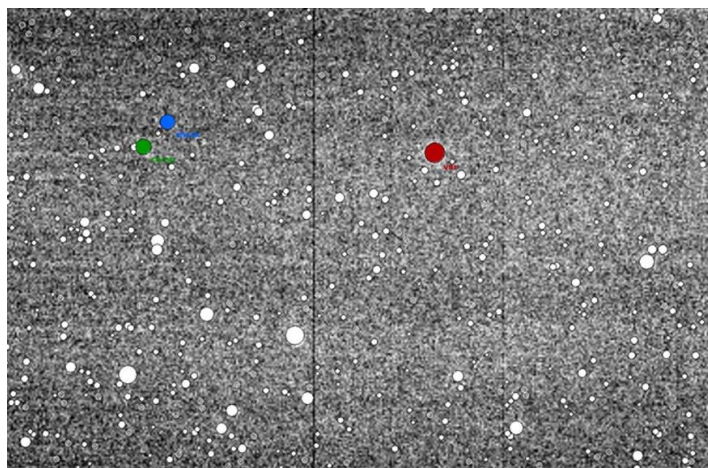

Figure 3: The selection of the comparison star and of the check star for the MW Com variable

Table 2: Observation nights of MW Com

Year	Month	Day	Start	End	No. of fits files
2016	March	17.	19:31	19:40	22
		24.	20:44	21:41	25
		31.	19:24	22:27	81
	April	07.	19:11	20:30	42
		12.	19:04	21:34	79
		21.	19:51	22:29	90
		26.	20:36	20:54	16
	June	06.	21:01	21:24	13
		07.	21:04	23:47	93
		22.	21:06	23:05	68
		23.	21:03	23:43	85
		28.	21:02	23:13	71
	July	04.	21:24	22:35	43
		06.	20:53	22:49	64
2017	March	26.	19:13	20:52	44
		27.	19:21	24:00	95
		28.	00:00	00:22	12
	April	1.	20:15	24:00	82
		2.	00:00	01:14	94
		24.	19:50	20:45	27

	May	2.	20:43	22:32	44
		17.	19:24	21:04	42
		18.	19:19	20:59	42
		28.	19:43	23:34	86
	June	1.	20:40	22:28	45
		3.	19:13	21:59	26
		26.	20:57	21:53	30
	July	3.	19:47	22:14	54
		7.	19:26	21:14	41
		8.	19:32	21:15	30

The weather conditions have been well and the sky had been clear for this variable too. The selection of the comparison star (3UC239-108915) and of the check star (3UC239-108919) is on the Figure 3.

In this case, we have obtained complete light curves in the filters B, V, R and I through the course of our observations. Moreover, we have obtained the complete light curve in the integral light too as we have one window of our filter wheel empty.
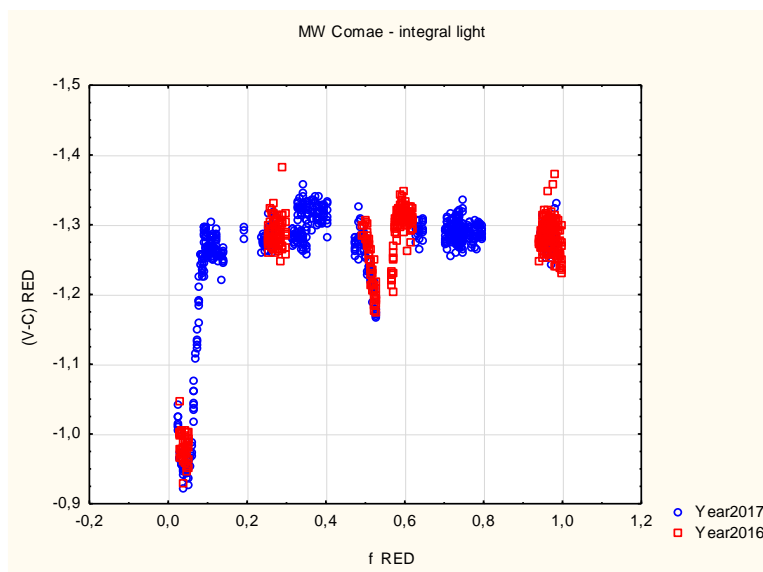

Figure 4: The common light curve (in the integral light too)

Finally, we allow us to stress that our results are of good quality ant they can be used in the next analysis. They can be used especially in the color indices analysis and in the analysis of the components of the variable star by the usage of the BM3 software.

Color indices and models

V477 Peg

We have supposed that the color indices will follow the changes of light curves or that they will form some kind of the light curve alone. However, we have found that the color indices are stable in the course of the period. As the example we are giving into the present paper the B – V phase diagram (Figure 5) and the B – R diagram (Figure 6).
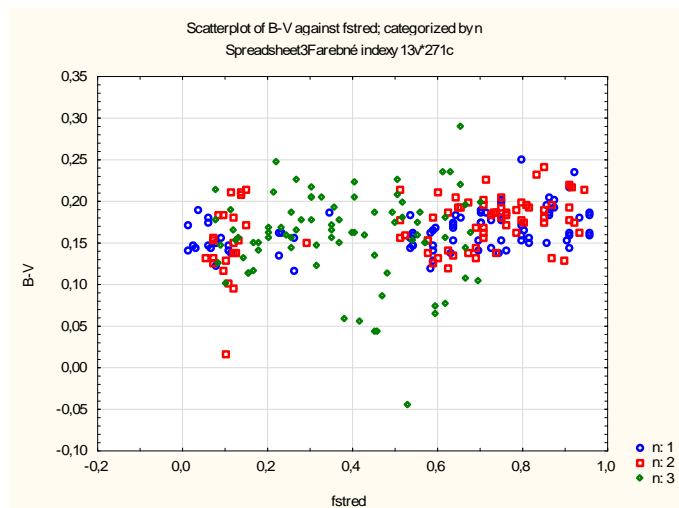

Figure 5: The B – V phase diagram for the V477 Peg. (The legend "n:i" there are the individual data from different nights)
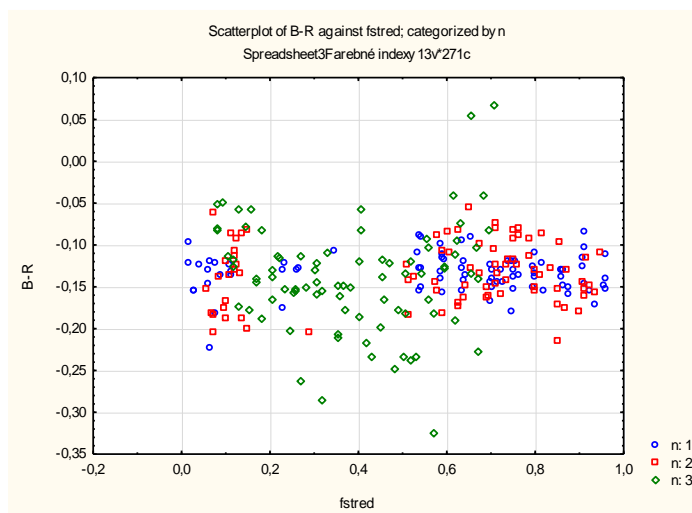

Figure 6: The B – R color indices phase diagram for the variable V477 Peg

MW Com

The situation with the color indices for the MW Com system is the same as for the V477 Peg. There are no changes with the phase. We give in this paper the Figure 7 for the B – V index and the Figure 8 for the B – I color index.
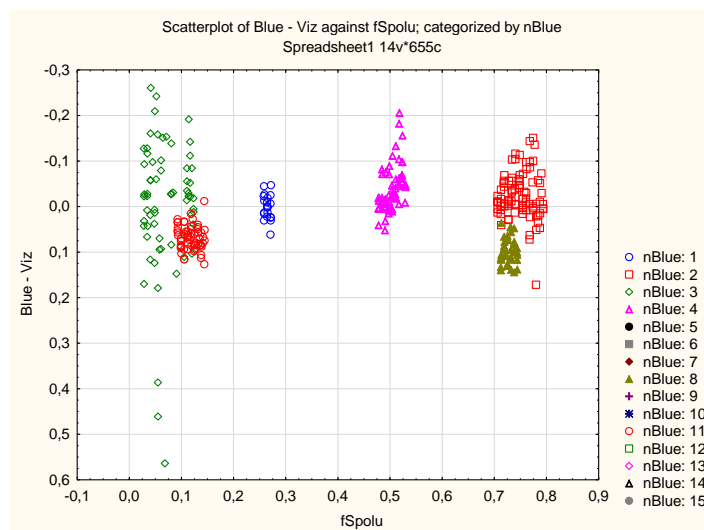

Figure 7: The B – V color index phase diagram for the variable MW Com
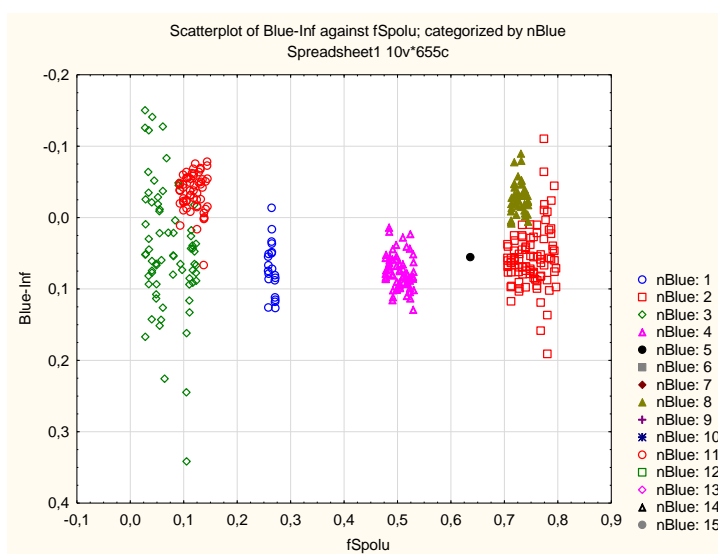

Figure 8: The B – I color index phase diagram for the variable MW Com

We have taken notice of rather great dispersion of the color indices on the Figure 7 and on the Figure 8. However, we are of the opinion that this dispersion is reflecting the dispersion of measurements and not real changes of the physical conditions inside the system. So or so we are planning to continue our observations of this system and we hope to confirm or reject the up mentioned working hypothesis with our future measurements.

Conclusions

We decided to try to realize the model of the both variable systems by the usage of the BM3 software. We feel the results as the excellent ones.
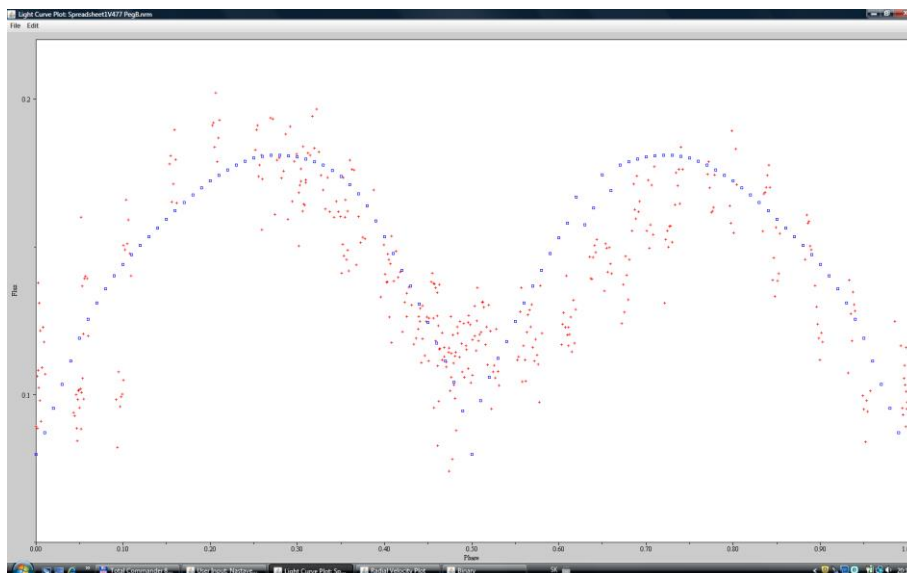

Figure 9: Model V477 Peg

If someone will to model the binary system by the usage of e.g. BM3 there is inevitable to select the appropriate parameters of the system. We are giving the Table 3 for these purposes.

Table 3: Parameters of the binary system V477 Peg

GEOMETRY	CYLINDRICAL	LATITUDE_GRID	20
INPUT_MODE	OMEGA_POTENTIALS	LONGITUDE_GRID	40
MASS_RATIO	1.4	WAVELENGTH	4400,0
OMEGA_1	4.5	TEMPERATURE_1	6000,0
OMEGA_2	4.0	TEMPERATURE_2	6000,0
GRAVITY_1	0	LIMB_1	0
GRAVITY_2	0	LIMB_2	0
REFL_1	0	REFL_2	0
THIRD_LIGHT	0	INCLINATION	90
NORM_PHASE	0.25	PHASE_INCREMENT	0.01
HAS_SPOTS	FALSE	USE_ADVANCED_PHASE	FALSE
HAS_DISK	FALSE	PSEUDOSYNC	TRUE
ROTATION_F1	1.0	ROTATION_F2	1.0
ECCENTRICITY	0.0	LONG_OF_PERIASTRON	0.0
ZERO_POINT_OF_PH.	0.0	USER_NORM_FACTOR	0.18

We decided not to go to details in the parameter selection, as according to our opinion the model is illustrative only. To be more precise we have not at our disposition the spectra of the system.

We see the situation for the variable MW Com very similar to the V477 Pegassi. The system of the MW Com we have determined as the classical algolid ant. This is why we did not included the model parameters into this

text. We see them very simple for this. Of course, we have included into our text the model diagram of this variable. It is depicted on the Figure 10 and we see in it the proof of the correctness of our simple model.
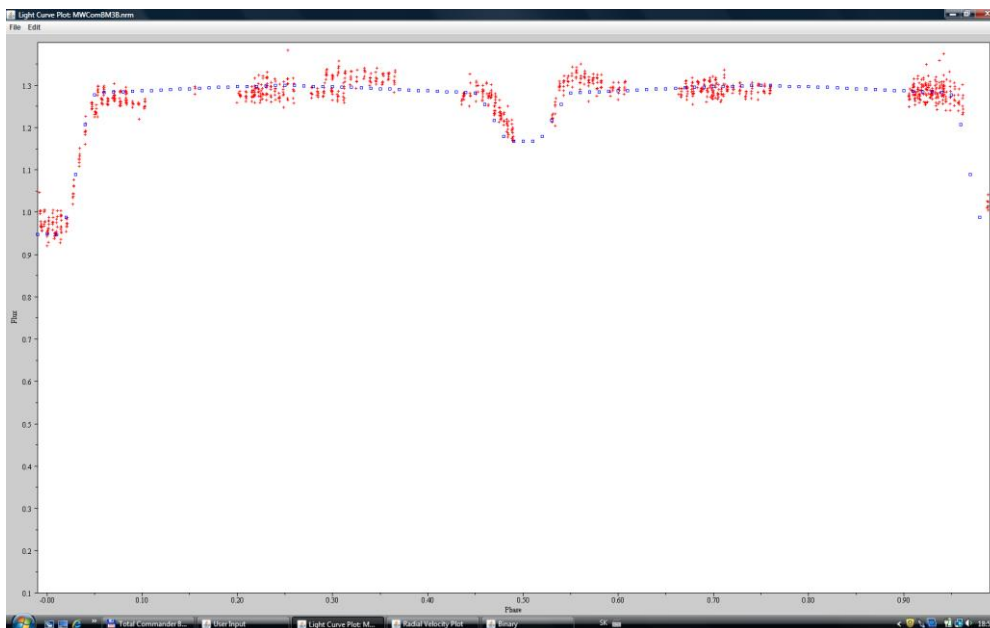

Figure 10: The model of the system MW Com

At the end of the conclusions, we allow us to declare that our observations have been correct and of the relevant quality and that our access to the problem of modeling the binary systems by the usage of the BM3 system had been correct and fruitful too.

Acknowledgement

References

Brandstreet, D. H., 2017, BM3, Eastern University, PA, www.euastronomy.com

Kazarovets, E. V. et al. 2012, Peremennye Zvezdy 32, No. 4

Kazarovets, E. V. et al. 2013 IBVS 6052

Motl, D., 2010, MuniWin V2.0.10, http://c-munipack.sourceforge.net

Pojmanski, G. 2002, Acta Astronomica 52 pp. 397 – 427

Raab, H., 2011, Astrometrica V4.6.6.394, http://www.astrometrica.at

Scientific Image Processing System (SIPS), 2016, Moravské Přístroje a.s. V3.3 32 bit (x86)

StatSoft, Inc, 2011, STATISTICA (data analysis software system), V10, www.statsoft.com

Automation of processing and photometric data analysis for transiting exoplanets observed with ESO NIR instrument HAWK-I

M. BLAŽEK [1,2] , P. KABÁTH [2], T. KLOCOVÁ [2], M. SKARKA [2]

(1)   Department of Theoretical Physics and Astrophysics, Faculty of Science, Masaryk University, Kotlářská 2,611 37 Brno, Czech republic

(2)   Astronomical Institute of the Czech Academy of Sciences, Fričova 298, 251 65 Ondřejov, Czech republic, martin.blazek@asu.cas.cz

Abstract: Nowadays, when amount of data still increases, it is necessary to automatise their processing. State-of-the-art instruments are capable to produce even tens of thousands of images during a single night. One of them is HAWK-I that is a part of Very Large Telescope of European Southern Observatory. This instrument works in near-infrared band. In my Master thesis, I dealt with developing a pipeline to process data obtained by the instrument. It is written in Python programming language using commands of IRAF astronomical software and it is developed directly for "Fast Photometry Mode" of HAWK-I. In this mode, a large number of data has been obtained during secondary eclipses of exoplanets by their host star. The pipeline was tested by a data set from sorting of the images to making a light curve. The data of WASP-18 system contained almost 40.000 images observed by using a filter centered at 2.09 μm wavelength and there is a plan to process other data sets. A goal of processing of WASP-18 and the other data sets is consecutive analysis of exoplanetary atmospheres of the observed systems.

Abstrakt: V dnešní době, kdy dat neustále přibývá, je stále nezbytnější automatizovat jejich zpracování. Dnešní moderní přístroje jsou schopny pořídit i desetitisíce snímků během jedné noci. Jedním z nich je HAWK-I, který je součástí VLT Evropské jižní observatoře. Tento přístroj pracuje v blízké infračervené oblasti. Ve své diplomové práci jsem se zabýval tvorbou pipeline zpracovávající jím pořízená data. Ta je napsána v programovacím jazyce Python s využitím příkazů astronomického softwaru IRAF přímo pro HAWK-I a jeho „Fast photometry mode". V tomto režimu vzniklo při pozorováních sekundárních zákrytů exoplanet hvězdami velké množství dat. Pipeline byla odzkoušena zpracováním jedné sady dat od roztřídění snímků po sestrojení světelné křivky. Data systému WASP-18 čítala bezmála 40 000 snímků s filtrem na vlnové délce 2.09 μm a v plánu je zpracování dalších sad. Cílem zpracování těchto a dalších snímků je následná analýza exoplanetárních atmosfér pozorovaných systémů.

Introduction

Eclipses give us valuable information about properties of an exoplanet and allow us to have a good picture about their characteristics and diversities. While primary eclipses (a planet covers a part of its host star), transits, tell us basic information about radius of the planet, inclination angle, etc., secondary eclipses (a planet is hidden beyond a star), occultations, give us rough idea about the planetary atmosphere.

Since radiation of a planet is mainly caused by reflected light of its host star and thus it is very low, flux decrease during an occultation is low as well. An other attribute of this is the fact that planets radiate mostly at longer wavelengths. It implies that to detect an occultation of an exoplanet, we need to use large telescopes with infrared or near-infrared instruments.

One of such instruments is High Acuity Wide-field K-band Imager, HAWK-I (*Kissler-Patig, 2008*), which is a part of one of four Very Large Telescopes situated on Paranal mountain in Chile. These telescopes are operated by the European Southern Observatory. HAWK-I works in near-infrared band between 0.85–2.5 μm. It contains four detectors, each with resolution 2048 px × 2048 px with 15-arcsec gap between the neighbouring detectors. Its field of view is 7.5' × 7.5' which is equal to 0.1064 px/arcsec. It is cooled within 80 K, so it produces very low dark current.

Except ordinary mode, HAWK-I can use *Fast Photometry Mode (Windowing)* for observations. Each of the detectors can be read-out in 16 vertical stripes and they can be also cut horizontally in any pixel according to setting of an observer. These type of images results into cube fits files which are 3D images of windows tiled together and then one put on each other. This mode thus enables to get a huge number of images during one night. Fast Photometry Mode is used for getting science and dark frames, flat-field frames are taken in ordinary mode.

There is many options, what part of each detector is read (setting of a user). Figure 1 shows four options as an example. The yellow, the purple, and the black rectangles show which area is read. All these areas are after read-out joined into a resulting image. The example with the dashed black line shows that a stripe of each detector is read and then joined same as the previous examples.
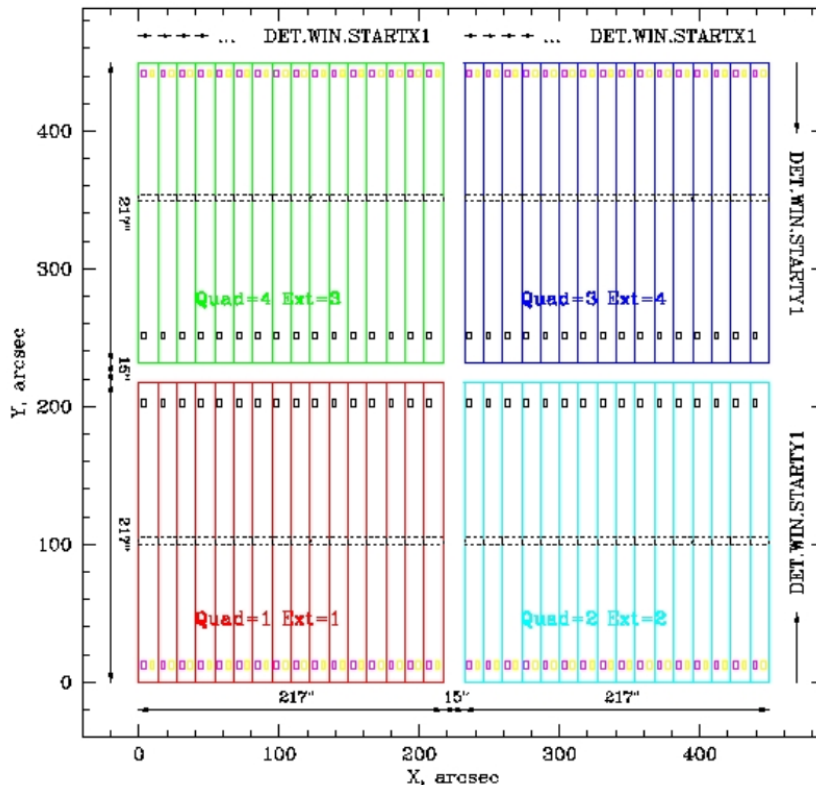

Figure 1: The priniple of Fast Photometry Mode of HAWK-I. Each of chips, as well as the vertical stripes, are drawn with a different colour. Four sets are represented here as examples. These are shown by yellow and purple colour and by two types of black lines. Taken from http://www.eso.org/

Secondary eclipses

When we observe secondary eclipses, we use emission photometry to find out some information about a planet's atmosphere. A light curve of an occultation (the depth), gives us a ratio of fluxes from a measured planet and its host star, so $\delta_{occ} \approx F_p / F_s$. The depth of the occultation is also dependent on radius of the planet (R_p) and the star (R_s): $\delta_{occ} = k^2 I_p / I_s$, where $k = R_p / R_s$ and I_p and I_s are averaged intensities of the disc of the planet and the star. The intensities can be approximated as blackbody radiators and then a wavelength dependent occultation depth is $\delta_{occ} (\lambda) = k^2 B_\lambda (T_p) / B_\lambda (T_s)$, where B_λ is the Planck function dependent on temperature of the planet and the star. We can see how depths of a transit and an occultation are connected because $\delta_{tra} = k^2$.

In practice, it means that a flux drop is usually in order of hundredths during transits and in order of thousandths during occultations.

Observation

To make a pipeline for automatic processing of HAWK-I Fast Photometry Mode images, a testing data set was used. These images have been obtained under proposal number 091.C-0488(A) during observational night 1.–2. 8. 2013, 4.12–10.38 UTC. The purpose of the observations was detection of a secondary eclipse of WASP-18 system with 2.09 μm filter (NB2090). The date set included 39.079 science images and 380 dark frames, all in 953 cube fits files, and 100 flat-field frames. Exposure times were 0.4 s, 0.5 s, 1.8 s and 2.0 s. The data which cover the occultation (and some time before and after it) are of the exposure time 0.4 seconds. This occultation observation was a part of program titled "Probing the atmospheres of the extreme exoplanets WASP-18b and WASP-19b".
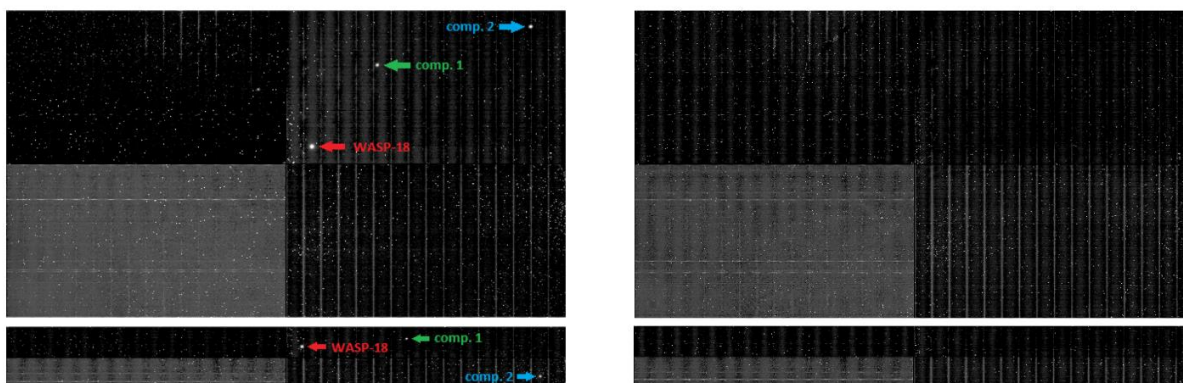
Figure 2: Two different-sized science frames with marked stars (left) of Fast Photometry Mode of HAWK-I and corresponding dark frames (right)
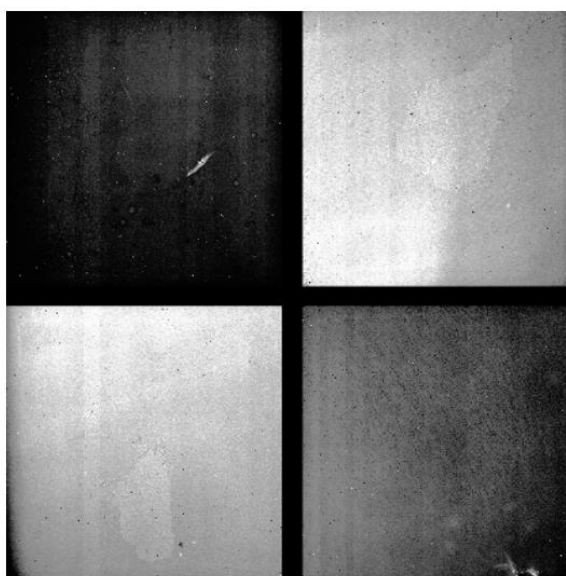

Figure 3: Flat-field frame of HAWK-I with its four detectors obtained by ordinary mode

Developed pipeline

For automatic processing of Fast Photometry Mode of HAWK-I a pipeline was developed. It consists of twelve scripts made in Python programming language. For the processing itself IRAF commands are used (Pyraf package of Python). It starts by an introductory script and after executing all commands a next script is launched at its end and this repeats throughout the whole pipeline. At some points co-operation with the user is required.

The structure of the pipeline is following:

• `pipeline.py`: the launching script, the option for using dark frames (▲) or not (▼):

    ▲ `darks.py`: dark frames processing, making of master dark frames;

    ▲ `darksStat.py` (optional): linearity graphs of particular detectors;

    ▲ `flatsD.py`: flat-field frames processing, making of master flat-field frames;

    ▲ `flatsStat.py` (optional): linearity graphs of particular detectors;

    ▲ `reductFlatsDarks.py`: data reduction, making of resulting images, preparing files for photometry.

    ▼ `flats.py`: flat-field frames processing, making of master flat-field frames;

    ▼ `flatsStat.py` (optional): linearity graphs of particular detectors;

▼ `reductFlats.py`: data reduction, making of resulting images, preparing files for photometry.

• `photometry.py`: doing photometry;

• `aperts.py`: choosing the best aperture for a light curve;

• `lightCurve.py`: making of the light curve, preparing a file for fitting routine;

• `std.py`: determining accuracy of measurements.

After cutting of the cube fits files and consecutive reduction using dark and flat-field frames, photometry of chosen stars within chosen apertures is done. Script `aperts.py` shows graphs aperture vs. flux so that a user could choose the best aperture for making a light curve. This works for each of measured stars separately and if a data set consists of images with various exposure times, it is separated as well. Then the light curve of an eclipse is produced and also a text file containing data used for the light curve is created. The user can choose time spans for that mentioned, the light curve need not be made of all points (images). For not showing outliers multiples of sigma (standard deviation) can be set. This script also makes a text file with needed data for MCMC fitting routine (*Gillon, 2009*). The last script calculates accuracy of measurements on given intervals outside the eclipse.
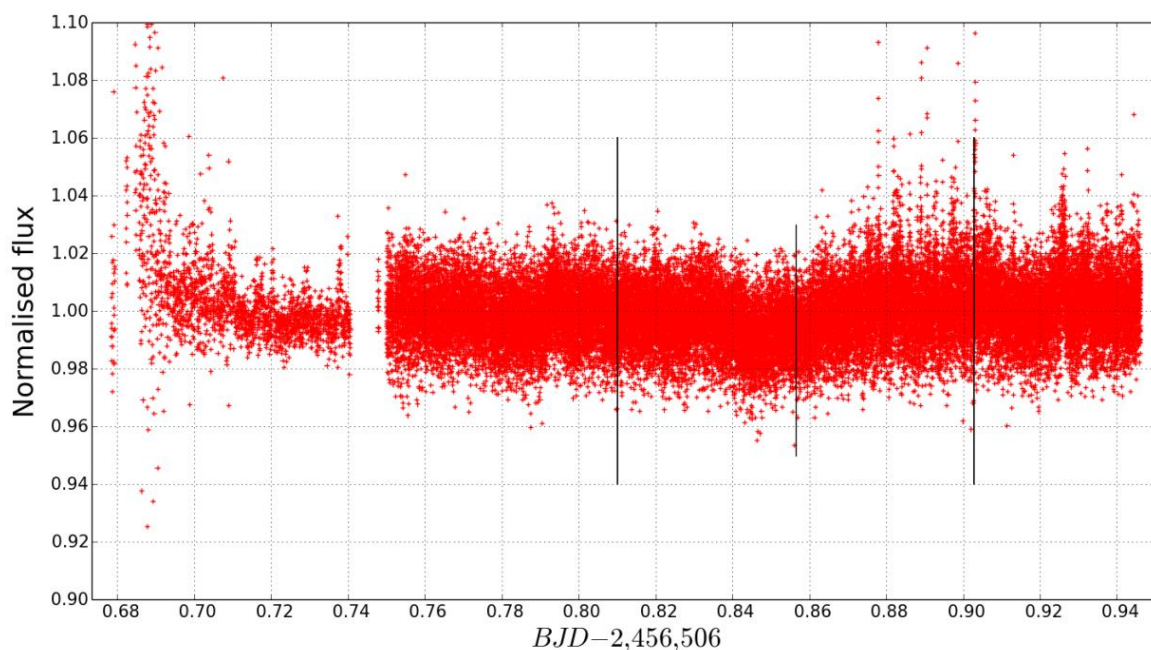
Output of the pipeline

Figure 4: Output of the pipeline. The light curve of the WASP-18 system during a secondary eclipse. The data were obtained 2. 8. 2013 with ESO VLT HAWK-I instrument using 2.09 μm filter. The vertical black lines represent the beginning, the center and the end of the eclipse

Discussion and conclusion

The pipeline was tested on the data set of WASP-18b occultation and although furher analysis is necessary, first results were obtained. A subject of further study will be thorough check of all possible effects. Next data sets of other hot Jupiters from ESO archive will be processed by the pipeline and then analysed to search for occultations and to study atmospheres of the chosen exoplanets.

Acknowledgement

References

Blažek, M.: Master thesis: Automation of processing and photometric data analysis for transiting exoplanets observed with ESO NIR instrument HAWK-I. Brno, Faculty of Science, Masaryk University, 2017.

Gillon, M., et al.: VLT transit and occultation photometry for the bloated planet CoRoT-1b. Astronomy & Astrophysics, ESO, 2009.

Kissler-Patig, M., et al.: HAWK-I: the high-acuity wide-field K-band imager for the ESO Very Large Telescope. Astronomy & Astrophysics, ESO, 2008.

Knutson, H. A.: A map of the day-night contrast of the extrasolar planet HD 189733b. Nature, volume 447, 183–186. Letters to Nature, 2007.

Nymeyer, S., et al.: Spitzer secondary eclipses of WASP-18b. The Astrophysical Journal, 2010.

Seager, S.: Exoplanets. Arizona (USA), The University of Arizona Press, 2010, ISBN 978-0-8165-2945-2.

Electronic source

http://www.eso.org/

Infrared Astronomy

J. Grygar [1]

(1)   Institute of Physics, Czech Academy of Sciences, Na Slovance 2, Prague, Czech Republic, grygar@fzu.cz

Abstract: Although infrared radiation was described by W. Herschel already in 1800, technical problems delayed its use in astronomy for 160 years. After the invention of a sensitive bolometer and semiconducting CCD arrays for very wide infrared window the progress in the field accelerated. Many high-altitude observatories started their work in the last three decades of XXth century and since 1983 space observatories became most important due to the fact that infrared radiation penetrates through opaque cold shells. Moreover, cosmological expansion of the Universe shifts the maximum of spectral energy of distant hot objects from ultraviolet to near infrared region. Infrared astronomy is also essential for improving our knowledge of the cold universe, particularly for studies about the birth of stars, planetary systems and galaxies.

Introduction

The so-called "calorific rays" were discovered by Sir William Herschel (1738-1822) in 1800 due to a simple and beautiful experiment with solar spectrum and a set of thermometers. Herschel in the process of calibration of thermometers discovered that the highest thermal response occurred beyond the red limit of the solar visible spectrum (Herschel 1800 abc). In 1878 Samuel Langley invented first infrared bolometer that could measure the intensity of infrared radiation with the relative precision of 10^{-5}.

The most important astrophysical outcome of the Max Planck's law (Planck 1901) was quite apparent: all blackbodies with effective temperatures in the interval 3 K – 3 kK emitted most of its electromagnetic energy in the infrared passband 1 mm − 0,7 μm. While optical passband UBVR has narrow width 1:2.4, infrared passband covers much wider wavelength ratio 1:1,400!

Great impetus for opening astronomy infrared window has happened during the World War II when military infrared detectors have been implemented. Soon after the war astronomers realized that the earth´s atmosphere is not fully transparent to infrared radiation above several μm. The transparency is better at higher geographical latitudes and is very good in highly elevated and extremely dry Antarctica. The infrared signal/noise ratio can be improved by passive or active cooling of the detector and/or the whole telescope. Another obstacle of infrared astronomy stems from expensive and sophisticated technology of infrared narrow-band and wide-band filters that must also stop all stray optical light. This review is based partly on data from my leaflet (Grygar 1986).

Fortunately, astronomy measurements on almost all places round the world could employ an absolute infrared standard represented by a bright red giant star Arcturus (α *Boo*; V = 0 mag; sp K1 III, effective temperature 4.35 kK; 3.5 M_O; +19° north; distance 11 pc). Monochromatic radiation fluxes for a star with 0 bolometric magnitude for different standard infrared filters are given in the Table 1. Table 2 summarizes the classification of infrared astronomy domains and Table 3 indicates the standard photometric systems in optical and infrared astronomy.

Table 1: Monochromatic infrared flux density for 0 mag star

Radiometric Passband	λ_{eff} [μm]	Monochromatic flux density [W m^{-2} μm^{-1}]	Limiting magnitude for 1.5m reflector
I	0.91	$8.3 \cdot 10^{-9}$	18
J	1.2	$3.4 \cdot 10^{-9}$	15
K	2.2	$4.1 \cdot 10^{-10}$	10
L	3.6	$6.4 \cdot 10^{-11}$	9
M	5.0	$1.8 \cdot 10^{-11}$	7.5
N	10.8	$9.7 \cdot 10^{-13}$	6
Q	21	$6.5 \cdot 10^{-14}$	3

Table 2: Classification of infrared astronomy domains

Infrared domain	λ_{eff} [µm]	Frequency range [THz]	Observatory locations
Near infrared [NIR]	1 – 5	300 – 60	Ground observatories
Mid infrared [MIR]	5 – 30	60 – 10	High-altitude observatories, aeroplanes
Far infrared [FIR]	30 – 300	10 – 1	Aeroplanes, balloons, sounding rockets
Submillimeter	300 – 1,000	1 – 0.3	Artificial satellites, high-altitude observatories

Table 3: Standard systems of optical and infrared photometry

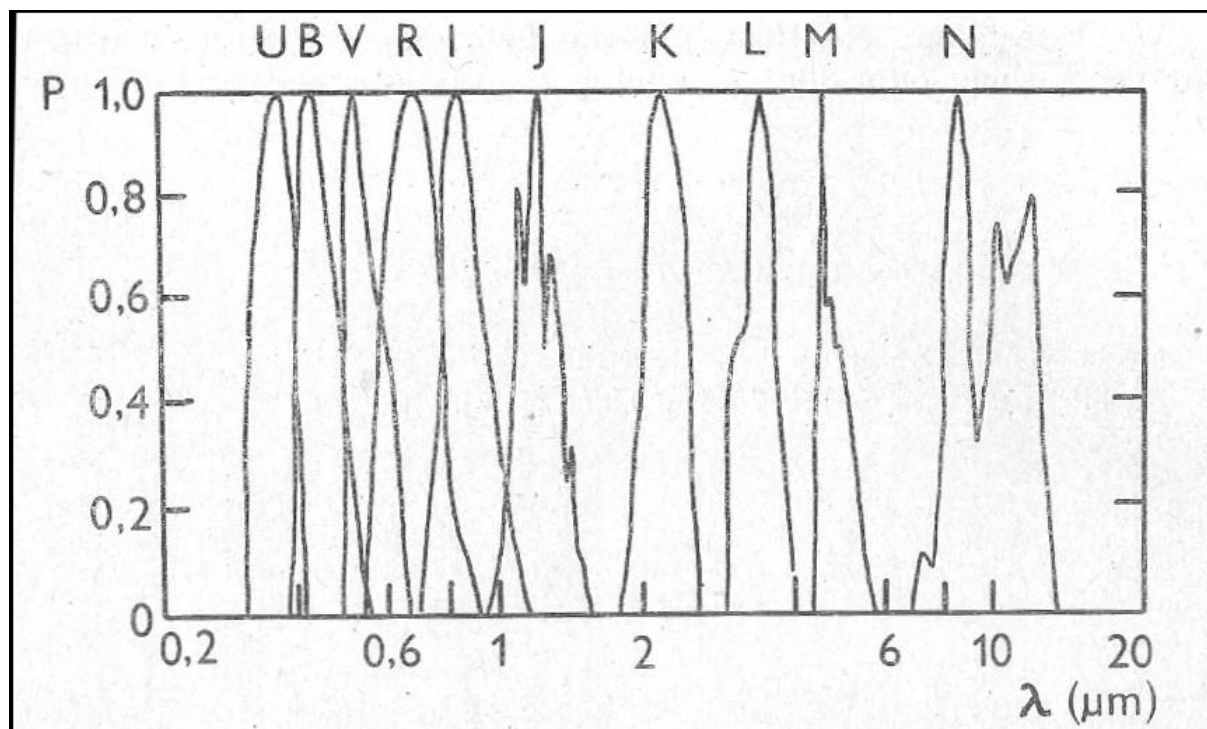| r	λ_{eff} [µm]	Width $\Delta\lambda$ [µm]	T max [K]	Method
U	0.365	0.066	7,900	Photoelectric photometry with photomultipliers, or standard photographic photometry with UBVR filters
B	0.44	0.10	6,600	
V	0.55	0.09	5,300	
R	0.70	0.21	4,100	
I	0.91	0.23	3,200	Photomultipliers, Si diodes, Special photographic emulsions
J	1.2	0.3	2,400	
H	1.65	0.4	1,750	PbS and InSb detectors
K	2.2	0.56	1,300	
L	3.6	0.7	800	
M	5.0	1.1	580	
N	10.6	4.3	270	Triple semiconducting chips [HgCdTe]
Q	21	7.5	138	

Figure 1: Spectral response of standard filters and atmosphere transparency in optical, NIR and MIR passbands

Why the infrared astronomy was so late?

First bolometers were not very sensitive in the whole IR domain, while observers and instruments themselves are intense radiators under room temperatures (passband N). For improving the signal to noise ratio it is absolutely necessary to cool the detector and possibly the whole instrument to liquid nitrogen [77 K] or helium [4 K] temperatures. This is tricky and expensive. First modern refrigerated Ga-doped germanium bolometer was constructed in 1961 for operational wavelengths $1 \div 100$ μm (Low 1961). Next great progress were triple compositions HgCdTe first imployed for detection of missiles, and than for the remote sensing of Earth from satellites. First HgCdTe arrays were manufactured as CCD chips with 32 x 32 pixels [1985]. However contemporary chips achieve the capacity 2048 x 2048 pixels. Helium cryostats are very complex machines due to superfluid behaviour of helium. Moreover this behaviour complicated the use of superfluid helium under weightlessness condition aboard spacecrafts.

High-altitude and South Pole observatories

First infrared observatory was erected by the University of Wyoming in 1977 at Jelm Mt. (2.9 km a. s. l.]. WIRO 2.3 m reflecting telescope is stil operational. Soon after United Kingdom opened 3.8m infrared telescope UKIRT at Mauna Kea, Hawaii (4.2 km a. s. l.) and NASA started there 3m infrared telescope IRTF. Further infrared facilities were during the eightees in Australia (3.9 m AAT, Siding Spring; 1.2 km a. s. l.), Arizona, California and Chile. From 2,000 infrared instruments are abundant at the largest optical telescopes, namely 8.2m VLT ESO telescopes at Cerro Paranal, and 10m Keck telescopes at Mauna Kea. Moreover, infrared telescopes operated remotely are now available on the Antarctica plateau near South Pole. During southern winter these instruments could operate continuously for almost half a year. Recently a high-altitude balloons are launched at the McMurdo polar station. Due to stable polar vortex the detectors could study infrared radiation of various objects for a fortnight and its multiplets. Polar vortex with this period of circulation gives the researchers the opportunity to studying various objects from the height up to 35 kms above sea level.

Moreover, NASA operated from 1970 sounding rockets with infrared detectors in the passbands $4 \div 27$ μm. During cummulative time of 30 mins the detectors covered the whole sky in four infrared filters. Since 1975 NASA operated also a high-altitude plane Kuiper Airborne Observatory (KAO) with infrared decettors for the whole passbands $1 \div 500$ μm. The aircraft Lockheed C-141A Starlifter accommodated with 0.9 m reflector operated in range up to 11 thousand km and altitude up to 14 km. It was very versatile instrument until 1995. The KAO discovered rings of Uranus, atmosphere of Pluto and mineralogy of the surface of Mercury. KAO also

studied the infrared radiation from centers of nearby galaxies, aftereffects of supernovae and it discovered organic molecules and water in interstellar clouds and stellar nurseries.

Infrared astronomy in space

First infrared spacecraft **IRAS** was launched in 1983 trough cooperative effort of the Netherlands, United Kingdom and USA. IRAS primary mirror with a diameter 570 mm was equipped with four-band infrared detectors and cooled to 2 K by a sophisticated refrigerator. During 10 months the observatory discovered 250 thousand infrared sources over the whole sky. As a bonus a mother minor planet Phaeton of a stable meteor shower Geminds was discovered. Since then astronomers used almost a dozen infrared space observatories:

COBE (NASA; Ø 190 mm)**: 1989-1993** (*Cosmic Background Explorer*): study of relic radiation and infrared background radiation.

ISO (ESA; Ø 0.6 m)**: 1995-1998** (*Infrared Space Observatory*; 1,7 K; $2.5 \div 240$ μm).

HST (NASA & ESA; Ø 2.4 m): **1997 - :** NICMOS (*Near-Infrared Camera & Multi-Object Spectrometer*). **2009** - : Camera WFC3 ($0.8 \div 2.1$ μm).

SST (NASA; Ø 0.85 m): **2003 -** (*Spitzer Space Telescope*); $3.6 \div 160$ μm; since V 2009 only 3.6 and 4.5 μm. Solar trailing trajectory.

Akari (= „light"; JAXA + ESA + J. Korea; Ø 0.7 m): **2006 – 2011:** ($1.7 \div 100$ μm).

Herschel (ESA; Ø 3.5 m): **2009 – 2013: (**$55 \div 672$ μm**).** Point L_2 (Earth – Sun).

WISE (NASA; Ø 0.4 m): **2009 – 2010** (*Wide-field Infrared Survey Explorer*): 4 bands ($3 \div 25$ μm).

SOFIA {NASA; DLR; ; Ø 2.5 m). **2010 - ?:** $0.3 \div 1\ 600$ μm (*Stratospheric Observatory for Infrared Astronomy*): range 12,000 km; altitude 13.7 km; continuous observation 8 h; flight duration 12 hrs. Very operative program for rare and unexpected phenomena.

NeoWISE (NASA; Ø 0.4 m): **2013 – 2017?:** (3.4 and 4.6 μm; potentially hazardous asteroids). Already >7 all sky surveys; >28 thousand objects in the Solar system; >70 PHA; 130 comets).

JWST (NASA; ESA; CSA; Ø 6.5 m): **2019?:** directed by J. Mather. First concept 1997 (Ø 8 m; start 2007; 0.5 G\$). 2011 almost cancelled. Now Ø 6.5 m; budget 9 G\$, Spectral coverage from orange colour to MIR passbands. Location L_2. 5 years lifetime.

Infrared cosmology

Modern cosmology studies the objects in their local time abou 500 million years after the big bang. Although the Universe was pretty hot in that times and therefore its thermal radiation has the maximum in the far ultraviolet at the Lyman limit (91 nm), we may observe the Lyman limit shifted to infrared part of the electromagnetic spectrum (1,470 nm). The largest redshift z = 11.09 observed with the HST camera WFC3/IR G141 belongs to a very young galaxy **GN-z11** at its age 414 million years after the Big Bang. Thus, JWST is designed to enter the era of infrared cosmology where we shall be able to discover the state of the Universe some 200 hundred millions years after the big bang. Surprises are, of course, welcome.

References

Grygar J., 1986, Kapitoly z astronomie 14, Infrared astronomy, Brno

Herschel W., 1800, Phil. Trans. R. Soc. Lond. 90, a) 239-254; b) 255-283; c) 284-292

Low F., 1961, J. Optical Soc. America 51, no. 11, 1300

Planck M., 1901, Ann. Phys. 309, no. 3, 553

GJ 3236 - radial velocity determination

J. Kára[1], M. Wolf[1], S. Zharikov[2]

(1)   Astronomical Institute, Charles University, V Holešovičkách 2, 180 00 Praha 8, Czech Republic,
kara@sirrah.troja.mff.cuni.cz

(2)   Instituto de Astronomia, Universidad Nacional Autonoma de Mexico, Apdo. Postal 877, Ensenada, Baja California,
22800 Mexico

Abstract: We present a new study of low-mass red-dwarf eclipsing binary GJ 3236 using spectroscopic data obtained by the 2.12-m telescope at the San Pedro Mártir Observatory. We resolved radial velocities of both components of the binary and improved determination of the physical parameters of the binary.

Introduction

Red dwarfs are cool stars with masses less then 0.6 solar mass. They represent the most abundant group of stars in our Galaxy. Because of their low luminosity, only about 20 eclipsing binary systems consisting of two M dwarfs are known. These systems represent a great opportunity for study of stellar flares, because by analysing spectroscopic and photometric data, we can determine parameters of their components with precision up to 1 %, which is sufficient for evolutional modelling of these stars.

Stellar flares are enormous releases of energy connected with magnetic activity of star, which manifest itself as rapid brightening of the star followed by slower decrease of brightness. Flare activity is common for red-dwarf stars, where massive convection can generate strong magnetic field. Magnetic field can manifest itself also in the form of spots on the surface of the stars and can affect the shape of the light curve, which can then vary over time.

We present a study of red-dwarf eclipsing binary GJ 3236 based on new spectroscopic data. This star was discovered to be an eclipsing binary by Irwin et al. (2009), who also determined parameters of this binary system. The flare activity of this star was addressed in recent papers by Parimucha et al. (2016) who observed 7 flares and by Šmelcer et al. (2017), who reported 78 observed flares.

Observations

Spectroscopic data were obtained at the San Pedro Mártir Observatory in Mexico with a 2.12-m telescope equipped with echelle spectrograph, which is operated by National Autonomous University of Mexico. The spectrograph is capable of a resolution of R ~18000 at wavelength of 500 nm and the spectra cover wavelengths from 360 nm up to 730 nm. Observations took place during three nights in November 2016 and 14 spectra with exposure time of 20 minutes were taken in total. Spectroscopic data were reduced using standard procedures in IRAF (iraf.noao.edu).

Radial velocity analysis

Radial velocities were obtained by fitting Hα emission line, which clearly consist of two separated peaks corresponding to the components of the binary system. Hβ emission line is also visible in the obtained spectra, but it is highly affected by the noise and therefore only Hα emission line was used for analysis. An example of observed Hα line is shown in Figure 1. The fitting was done using program IRAF and data were fitted by model

Table 1: Radial velocities for primary component (v_1) and secondary component (v_2).

HJD - 2450000	v_1 [km/s]	v_2 [km/s]
7707.85313	58.43	-31.06
7707.86729	64.31	-46.20
7707.88142	72.66	-57.58
7707.89801	81.54	-64.18
7709.80131	-35.35	86.85
7709.81543	-43.91	90.62
7709.82955	-52.01	99.42
7709.84381	-58.02	109.45
7709.85805	-65.15	115.88
7709.87252	-69.51	119.74
7710.79411	-42.47	88.82
7710.80825	-35.04	79.25
7710.82238	-26.96	69.47
7710.83654	-15.56	56.56

consisting of two Voigt profiles and a linear continuum. Derived radial velocities where then corrected for the heliocentric correction, which was computed also by using program IRAF. Adjusted radial velocities for both components are listed in Table 1.

Previously published data by Irwin et al. (2009) were also used for radial velocity analysis, namely radial velocities derived by comparison with spectra of star GJ 856A, which were also based on Hα emission line. Radial velocities of the primary component from both data sets were used to determine period using program Period04 (www.univie.ac.at/tops/Period04). Thanks to the long time passed between these observations, the

Table 2: Parameters derived from fitting

Parameter	Value and error	Irwin et al. (2009)
Period [days]	0.77125419(90)	0.7712600(23)
K_1 [km/s]	88.02(48)	88.48(33)
K_2 [km/s]	113.74(70)	114.71(49)
γ [km/s]	13.69(28)	13.87(19)
$q = M_2/M_1$	0.774(11)	0.7713(45)

accuracy of period determination is improved, compared to period derived from a single data set. According to Irwin et al. (2009) the eccentricity of the binary system is close to zero and one can assume a circular orbit. This assumption was used for radial velocities fitting, where data for each component were fitted by a sine curve. The best fit is shown in Figure 2 and parameters derived from the fit are presented in Table 2, where K_1 and K_2 stand for radial velocity amplitude of primary and secondary component, γ stands for radial velocity of the binary system a q stands for mass ratio of the binary system. Parameters derived by Irwin et al. (2009) are listed also in Table 2 for comparison.
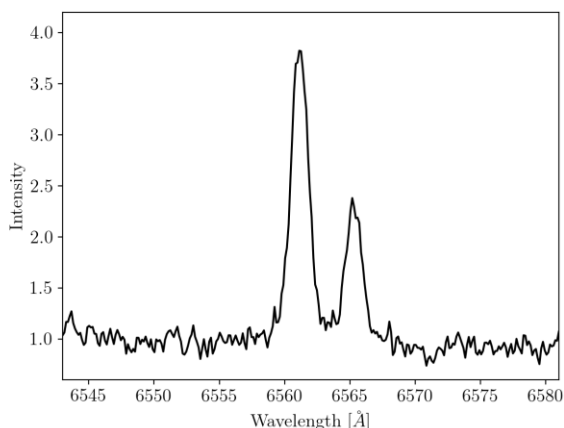

Figure 1: Spectrum of GJ 3236 showing the region around Hα emission line, which was used for the radial velocity analysis. The spectrum was taken during phase 0.19.
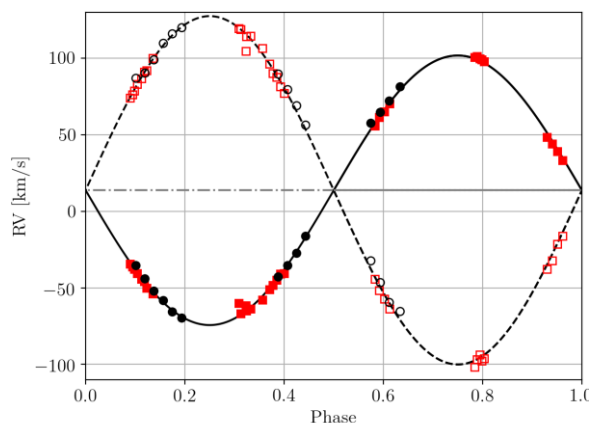

Figure 2: Phase-folded radial velocities for GJ 3236 system. Red squares represent data published by Irwin et al. (2009), black circles represent data from table 1. Filled symbols stand for primary component and empty symbols stand for secondary component. Velocities were phase-folded with period of 0.77125419 days.

Conclusions

We used spectroscopic observations to determine the radial velocities of both components of the binary star GJ 3236. We then determined parameters of this system by fitting newly obtained radial velocities and previously published ones. These parameters will be used for further study of this system, which will account also for the photometric observation.

Acknowledgement

References

Irwin, J. et al. 2009, ApJ, 701, 1436

Parimucha, Š., Dubovský, P.,Vaňko, M., & Čokina, M. 2016, Ap&SS, 361, 302

Šmelcer, L., Wolf, M., Kučáková, H., et al. 2017, MNRAS, 466, 2542

Recent photometry of selected symbiotic stars

M. VRAŠŤÁK[1,2]

(1)   Private observatory Liptovská Štiavnica (LSO), Kľučiny 457/74, Slovakia, mvrastak@gmail.com

(2)   Variable Star and Exoplanet Section of the Czech Astronomical Society, Vsetínská 941/78,

Valašské Meziříčí, Czech Republic

Abstract: A new multicolour (BVRcIc) photometric observations of symbiotic stars UV Aur, YY Her, V443 Her, V1016 Cyg, PU Vul, V407 Cyg, V471 Per and suspected symbiotic stars ZZ CMi, NQ Gem, V934 Her, V335 Vul, V627 Cas is presented. The data were obtained from 2016 October to 2018 January by the metod of classical CCD photometry. The monitoring program is still running, so on this paper partial light curves are presented.

Introduction

The aim of this work is the long-term monitoring of selected symbiotic stars and possible symbiotic objects, mainly observations of their symbiotic activity (outbursts, flickering) and improve the precission of the orbital photometric ephemerides and pulsational periods for symbiotic Miras.

Observations and reductions

CCD photometry was obtained at the Liptovská Štiavnica Observatory (LSO). A CCD camera MII G2-1600 and a Johnson-Cousins set of filters were mounted at the Newtonian focus of a 0.28-m and 0.35-m telescope respectively. The chip of the camera is KAF 1600 (16 bit), with dimensions of 13.8×9.2mm or 1536×1024 pixels. The pixel size is 9×9 μm and the scale 1".16/pixel. The readout noise was 12 ADU/pixel and the gain 1.5 e-/ADU. All frames were dark subtracted and flat fielded. Photometry was made with MuniWin routines. The differential magnitudes of the variables were calculated using transform coefficients into the standard Johnson-Cousins photometric magnitudes.

Table 1: Data for the measured symbiotic stars and suspected symbiotic stars

Symbiotic stars							
Star	V mag	α(2000)	δ(2000)	Orbital photometric ephemerides	Eclipse	Pulsation ephemerides for Miras	Type
UV Aur	8.5	05 21 48.8	+32 30 43.1			Max=2441062+395.42*E	
YY Her	12.8	18 14 34.3	+20 59 20.0	Min=2448945+590*E	no		ZAnd
V443 Her	11.5	18 22 08.4	+23 27 20.0	Min=2443660+594*E	no		
V1016 Cyg	11.2	19 57 04.9	+39 49 33.9			Min=2444852+478*E	SyN
PU Vul	11.6	20 21 12.0	+21 34 41.9	Min=2444550+4900*E	yes		SyN
V407 Cyg	14.0	21 02 13.0	+45 46 30.0			Max=2429710+745*E	
V471 Per	13.0	01 58 49.6	+52 53 48.9				
Suspected symbiotic stars							
ZZ CMi	9.9	07 24 13.9	+08 53 51.7				
NQ Gem	7.9	07 31 54.5	+24 30 12.5				
V934 Her	7.8	17 06 34.5	+23 58 18.5				
V335 Vul	11.8	19 23 14.2	+24 27 40.2			per=342 d	
V627 Cas	12.9	22 57 41.2	+58 49 14.9			per=466 d	

Table 2: Magnitudes of the comparison stars used for each targets

Name	V	B-V	V-Rc	Ref
Comparison star in the field of UV Aur				
TYC 2394 687	8.707	1.107	0.654	4,5
Comparison star in the field of YY Her				
UCAC4-556-067825=120	12,040	0.632	0.362	2,4
Comparison star in the field of V443 Her				
UCAC4-568-066765=115	11.547	1.179	0.650	1,4
Comparison star in the field of V1016 Cyg				
„a"	12.314	0.552	0.334	3
Comparison star in the field of PU Vul				
„b"	12.517	0.613	0.359	3
Comparison star in the field of V407 Cyg				
UCAC4-680-094809=118	11.822	0.739	0.405	1,4
Comparison star in the field of V471 Per				
UCAC4-715-015241	10.739	0.313	0.140	2
Comparison star in the field of ZZ CMi				
„γ"	10.572	0.893	0.534	3
Comparison stars in the field of NQ Gem				
UCAC4-573-040703=108	10.829	1.180	0.683	4,5
„c"	10.752	0.342	0.275	3
Comparison stars in the field of V934 Her				
„a"	10.189	0.584	0.376	3
Comparison stars in the field of V335 Vul				
UCAC4-573-086386	11.958	0.596	0.331	1
Comparison stars in the field of V627 Cas				
UCAC4-745-079996	11.966	0.527	0.262	1

Refs: 1. Henden – Munari I (2000), 2. Henden – Munari II (2001), 3. Henden – Munari III (2006), 4. AAVSO database (B and V magnitude), 5. this paper (Rc magnitude)

Light curves of the measured objects
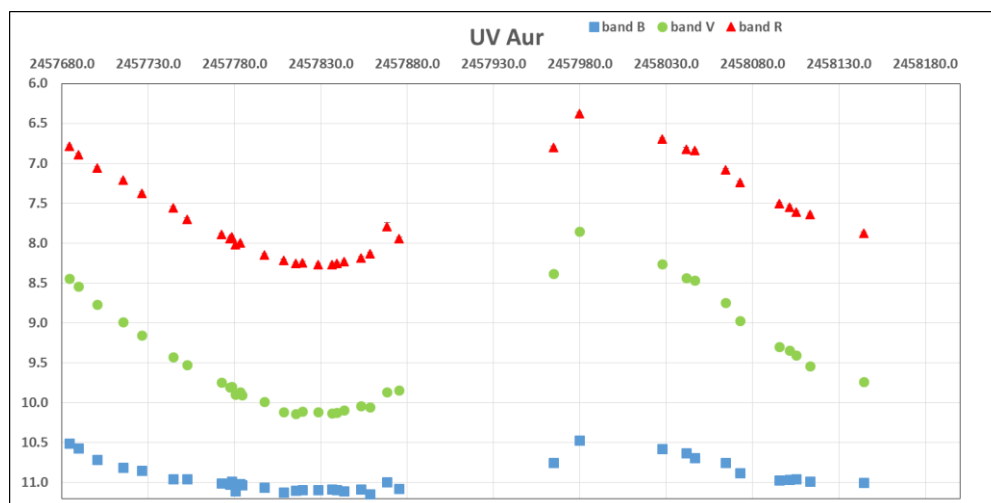
Figure 1: The light curve of UV Aur obtained from JD 2457684 to 2458144.
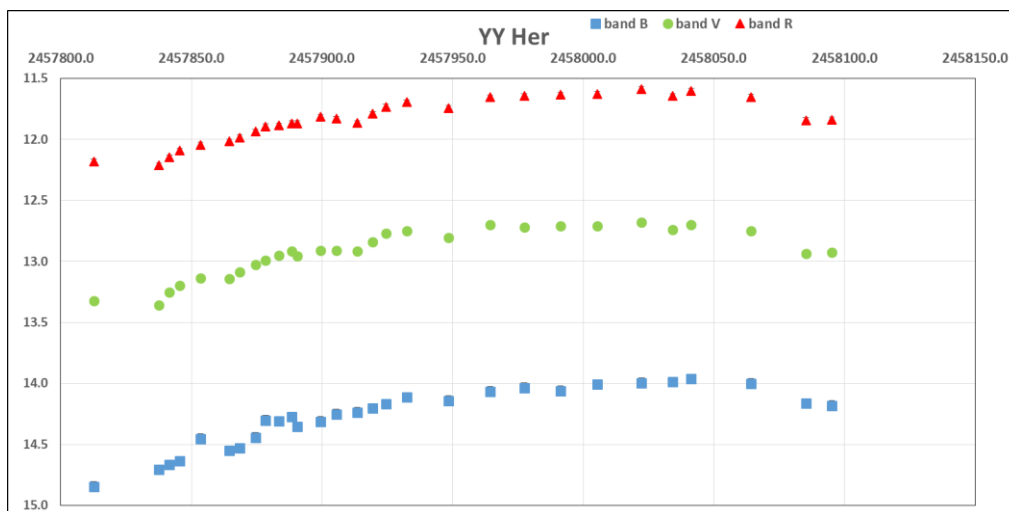
Figure 2: The light curve of YY Her obtained from JD 2457812 to 2458095.
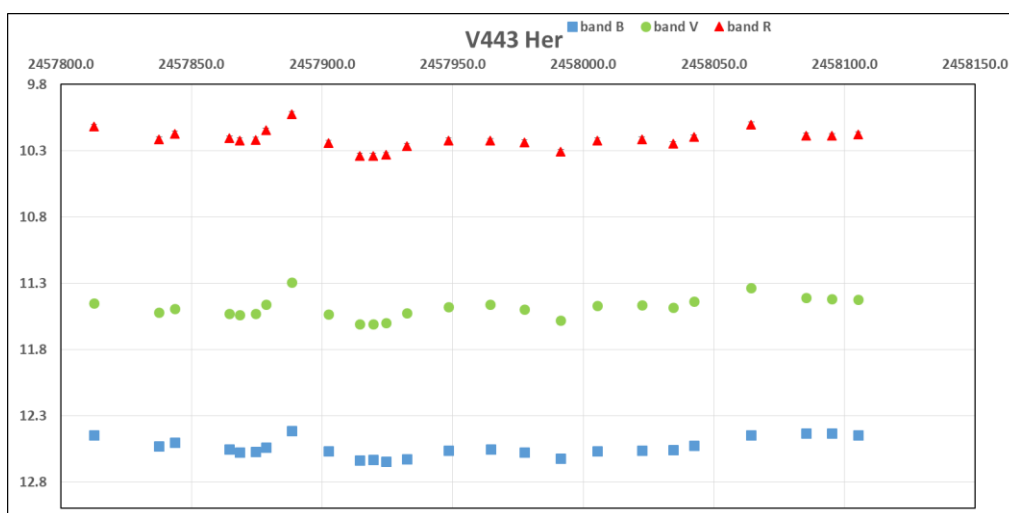

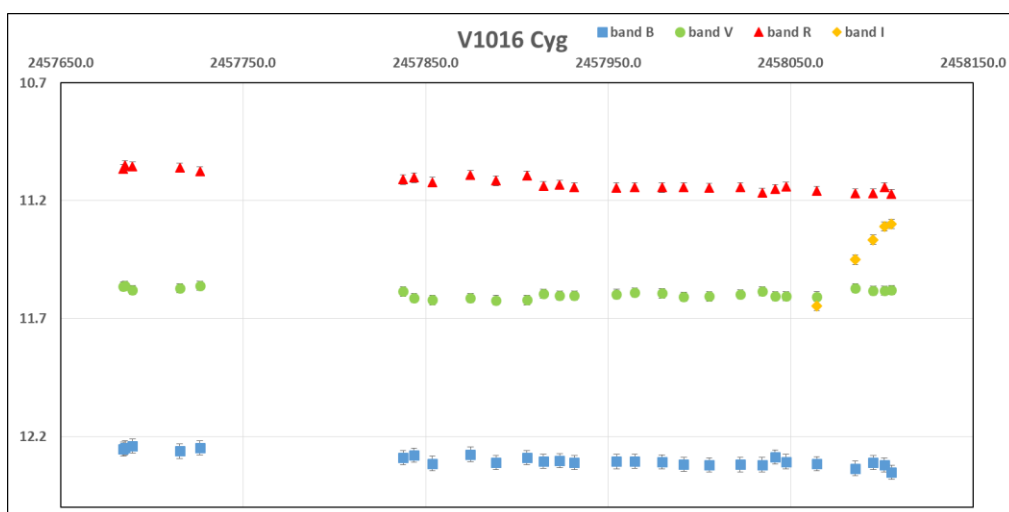**Figure 3:** The light curve of V443 Her obtained from JD 2457812 to 2458105.

Figure 4: The light curve of V1016 Cyg obtained from JD 2457684 to 2458105. Comparison star "a" R-Ic = 0.315.
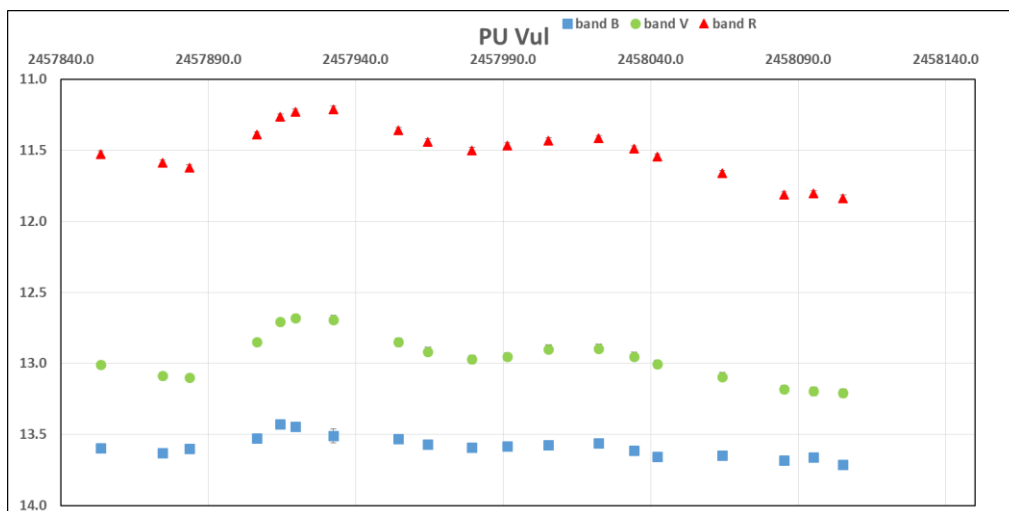
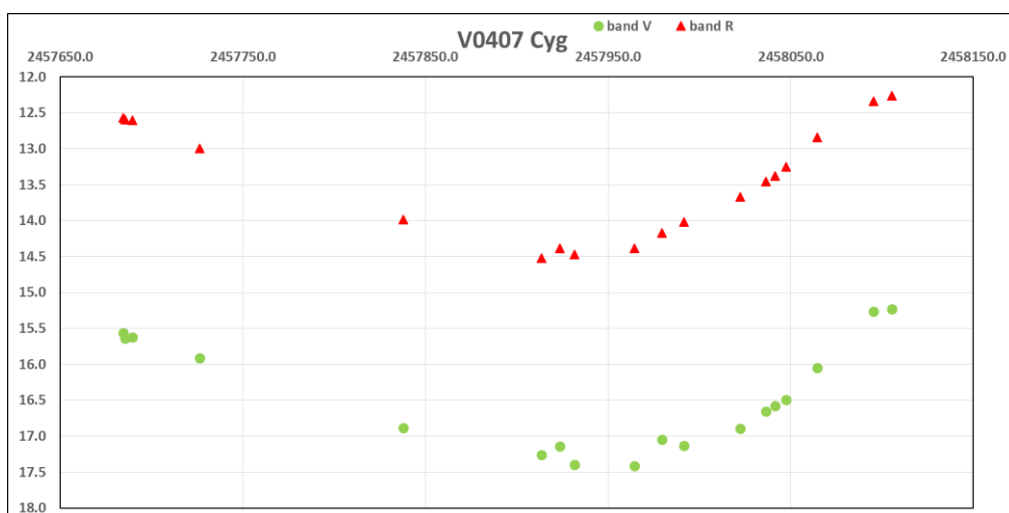**Figure 5:** The light curve of PU Vul obtained from JD 2457853 to 2458105.

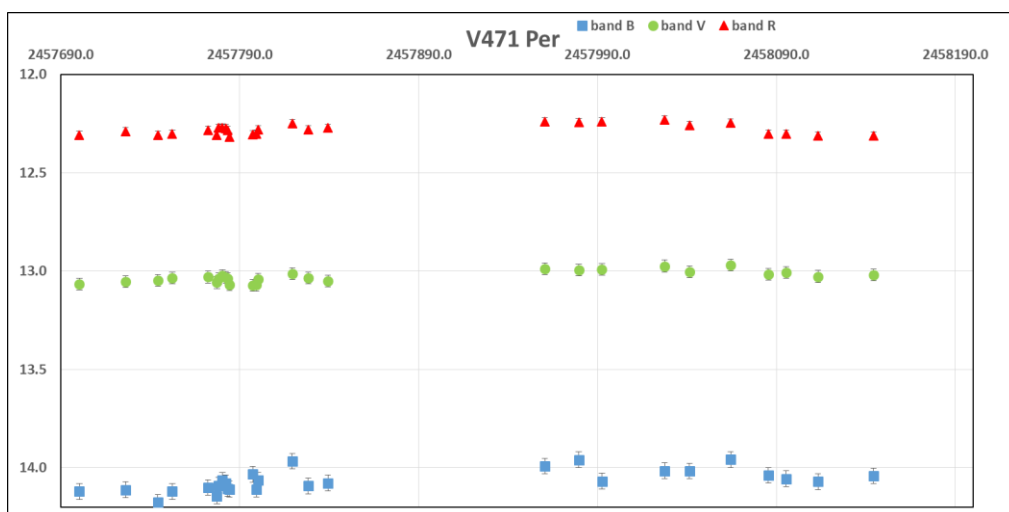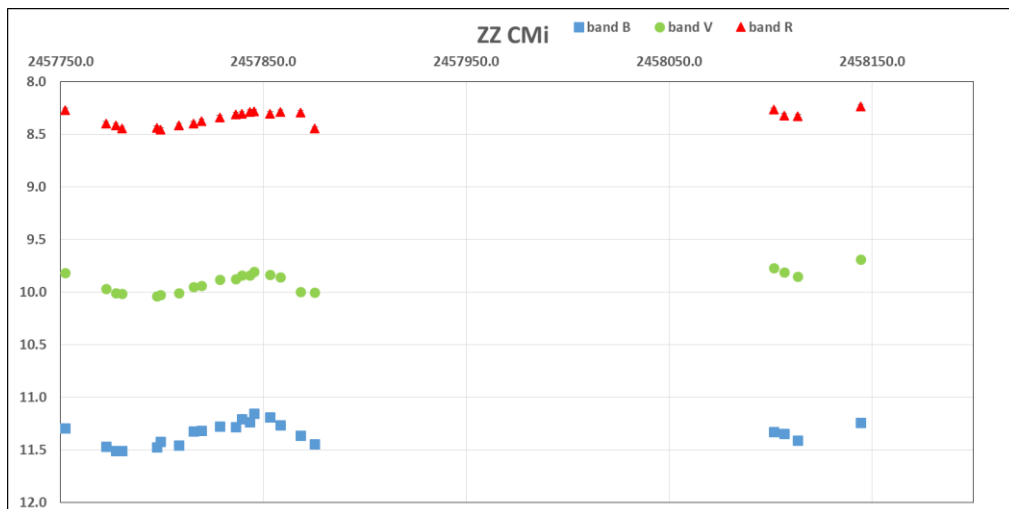**Figure 6:** The light curve of V407 Cyg obtained from JD 2457684 to 2458105.

Figure 7: The light curve of V471 Per obtained from JD 2457700 to 2458144.

Figure 8: The light curve of ZZ CMi obtained from JD 2457752 to 2458144.
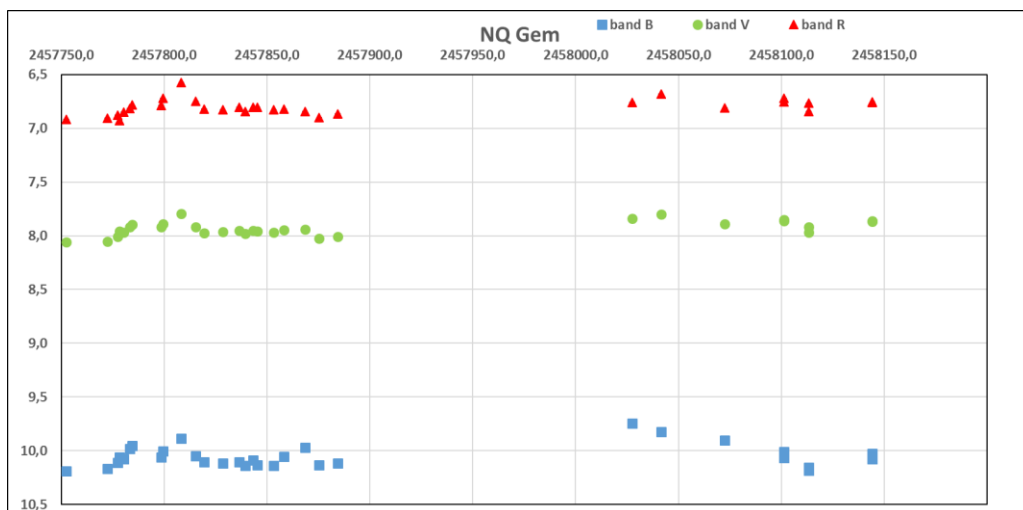

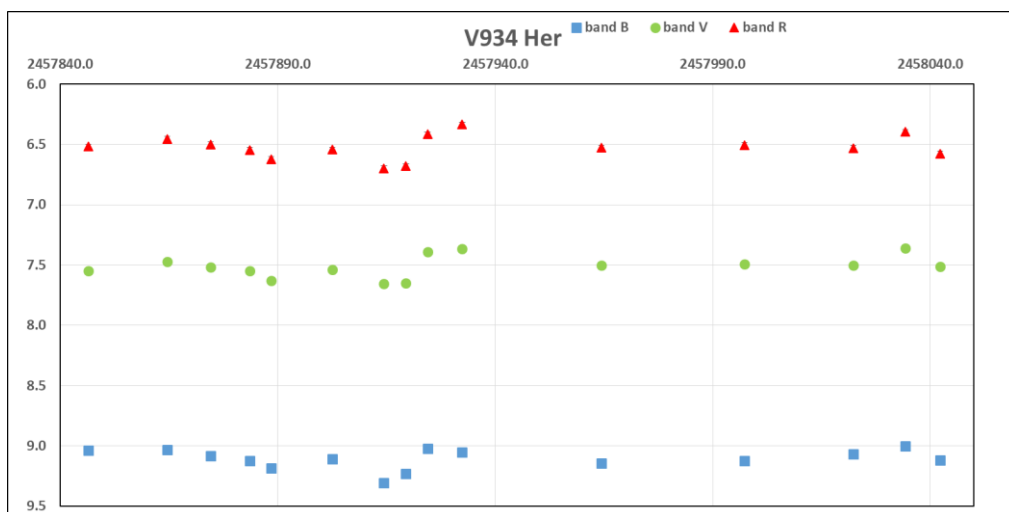**Figure 9:** The light curve of NQ Gem obtained from JD 2457752 to 2458144.

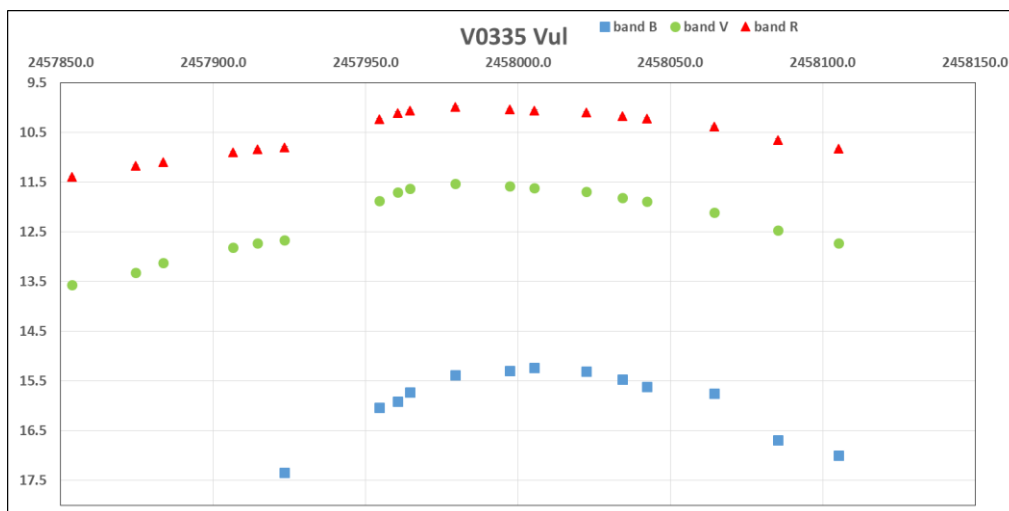**Figure 10:** The light curve of V934 Her obtained from JD 2457846 to 2458042.

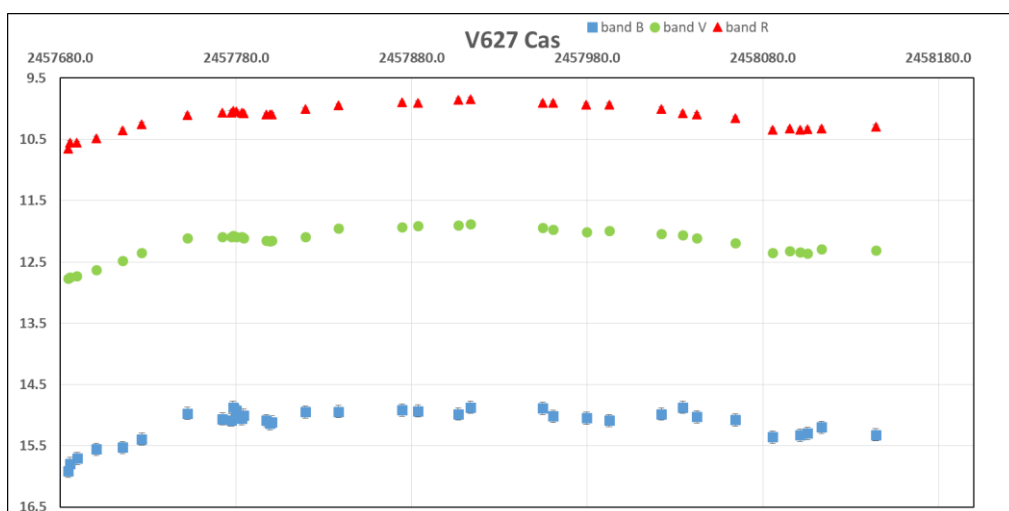**Figure 11:** The light curve of V335 Vul obtained from JD 2457846 to 2458042.

Figure 12: The light curve of V627 Cas obtained from JD 2457684 to 2458144.

References

A.Henden, U.Munari, UBV(RI)C photometric comparison sequences for symbiotic stars I, II, III

A.Skopal et al., Recent photometry of symbiotic stars – XIII

A.Skopal et al., Photometry of symbiotic stars – an international campaign VI

Chevalley et al., Sky Charts

K.Belczynski et al., A catalogue of symbiotic stars 2008

MuniWin, D. Motl 2012

The international Variable star index – AAVSO Zacharias et al., UCAC4 star catalog

U. Mürset and H.M. Schmid, Spectral classication of the cool giants in symbiotic systems

Eccentric binaries – still interesting targets

P. ZASCHE[1]

(1)   Astronomical Institute, Charles University, Faculty of Mathematics and Physics, CZ 180 00, Praha 8, V Holešovičkách 2, Czech Republic, zasche@sirrah.troja.mff.cuni.cz

Abstract: Eccentric binaries still provides us with valuable results and new observations of these systems are welcome. Especially these ones never analysed before should be observed for their light curves and minima.

Abstrakt: Excentrické dvojhvězy stále představují vítaný zdroj informací o hvězdách a jejich parametrech. Zvláště ty, které ještě nebyly podrobně zkoumány má smysl pozorovat: jejich světelné křivky i okamžiky minim.

Introduction – eccentric binaries

Eclipsing binaries are well-known to provide us the superb precise parameters of masses, radii, temperatures, etc. when dealing with really good photometry and spectroscopy (see Southworth 2012). However, these stars can also be used for statistical studies of stellar parameters, studying of stellar populations, calibrating the evolution models, or revealing the formation mechanism of their origin.

Focusing in more detail on the eccentric binaries, we can also study some other phenomena. Besides the classical analysis of apsidal motion in these systems (e.g. Giménez & García-Pelayo 1983), also a so-called period-eccentricity relation can be studied. Such a distribution of eccentricities with respect to the orbital period can tell us something about the formation scenario (Tokovinin 2008, or Kiminki & Kobulnicky 2012). Is the formation of binaries and multiples solely a matter of fragmentation, accretion, or some N-body dynamics? Or maybe a fruitful combination of all these mechanisms? Is the subsequent orbit migration crucial for explaining the observed orbital properties of binaries and multiples? The distribution of eccentricity can provide us strong constraints on the star forming theories and our result can be compared with the stellar formation models and the N-body simulations.

Observations – are welcome

Due to this reason, we would like to encourage the amateur observers for their new observations of eccentric binaries, which lack of new data. Many new eclipsing binaries were found only as "by chance" discoveries by amateur astronomers, and several of them are also the eccentric ones. New catalogue of CzeV discoveries published recently (Skarka et al. 2017) lists many such examples, i.e. CzeV 270, CzeV 364, CzeV 451, etc. Hence, discovering any such new eccentric binary provides us with a possibly very interesting system. Only after detailed light curve and O-C diagram analyses one is able to obtain the orbital eccentricity for these new systems and to plot these data into the period-eccentricity diagram.

For some of the newly discovered eccentric systems their good data are still missing. It means that obtaining the whole light curve and also several times of eclipses during a few-year period would be very welcome. Many of these stars are on the northern hemisphere, are of suitable brightness, have adequately short periods. Hence, this would be the very suitable observing program for amateur observers and these data would be publishable.

Period – eccentricity relation

Having the set of data for period and eccentricity from different sources, one can plot these on the diagram. See the Figure 1 below, where the data points from different catalogues were added together. The catalogue with the longest periods is the visual binary catalogue by Mason & Hartkopf (2007), while the spectroscopic catalogue by Pourbaix et al. (2004) has the orbital periods significantly shorter. These data are compared with the latest catalogue of eccetric eclipsing binaries published by Bulut & Demircan (2007), which comprises of only 108 systems with known periods and apsidal motions. As one can see, these binaries fills mostly only the area between 1 and 50 days. These are the typical periods of eccentric eclipsing binaries before the start of Kepler, OGLE and other large photometric missions.

However, what can be seen there is the tendency of orbital eccentricity becoming lower for shorter periods. This is the effect of orbital circularization in time, which should play a role in every eccentric binary. However, the time scales are usually rather long, and that is the reason why we see so many eccentric binaries on the sky. The rough estimation of probable colliding orbit is plotted in Fig.1 with the magenta curve.
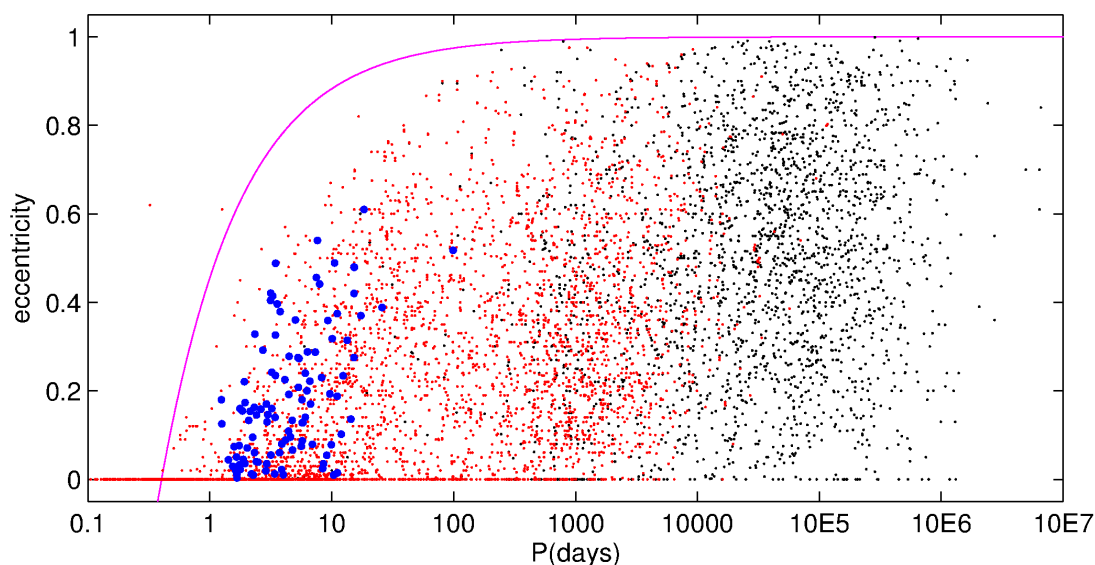
Figure 1: Period – eccentricity diagram of stars published in Pourbaix et al. (2004) in red, Mason & Hartkopf (2007) in black, in comparison with the eccentric eclipsing binaries from the catalogue by Bulut & Demircan (2007) in blue. The magenta line represents some rough estimation of stability limit.

Discussion and Conclusion

Eccentric binaries should be observed not only for their apsidal motion, which is usually rather slow. Also their complete light curves deserved our attention, because the proper modelling can only be carried out using good-quality data. Having the model of the binary, the derived orbital eccentricity together with the orbital period can tell us something about the stability of the system, its origin, or circularization times.

Acknowledgement

References

Bulut, I., & Demircan, O. 2007, MNRAS, 378, 179

Giménez, A., & García-Pelayo, J.M. 1983, Ap&SS, 92, 203

Kiminki, D. C., & Kobulnicky, H. A. 2012, ApJ, 751, 4

Mason, B.D., & Hartkopf, W.I. 2007, Binary Stars as Critical Tools & Tests in Contemporary Astrophysics, IAU Symposium 240, 133

Pourbaix, D., Tokovinin, A.A., Batten, A.H., et al. 2004, A&A, 424, 727

Skarka, M., Mašek, M., Brát, L., et al. 2017, OEJV, 185, 1

Southworth, J. 2012, Orbital Couples: Pas de Deux in the Solar System and the Milky Way, 51

Tokovinin, A. 2008, MNRAS 389, 925

Z CVn – Still mysterious

M. SKARKA[1,2,3], J. LIŠKA[2,4], R. DŘEVĚNÝ[2], Á. SÓDOR[3], T. BARNES[5] & K. KOLENBERG[6,7]

(1) Astronomical Institute of Czech Academy of Sciences, Fričova 298, CZ-251 65 Ondřejov, Czech Republic,
marek.skarka@asu.cas.cz

(2) Variable Star and Exoplanet Section of the Czech Astronomical Society, Vsetínská 78, CZ-757 01 Valašské Meziříčí,
Czech Republic

(3) Konkoly Observatory, Research Centre for Astronomy and Earth Sciences, Hungarian Academy of Sciences, Konkoly
Thege Miklós út 15-17, H-1121, Budapest, Hungary

(4) Central European Institute of Technology - Brno University of Technology (CEITEC BUT), Purkyňova 656/123, CZ-
612 00 Brno, Czech Republic

(5) The University of Texas at Austin, McDonald Observatory, 1 University Station, C1402, Austin, TX 78712, USA

(6) Institute of Astronomy, KU Leuven, Celestijnenlaan 200D, B-3001 Heverlee, Belgium

(7) Physics Department, University of Antwerp, Groenenborgerlaan 171, B-2020 Antwerpen, Belgium

Abstract: We comment on short- and long-term pulsation period variations of Z CVn, a classical RR Lyrae star with the Blazhko effect. Z CVn shows cyclic-like O-C diagram that can be interpreted as a consequence of binarity throught the light travel time effect. We show that this hypothesis is false and that the observed long-term period variations must be caused by some effect that is intrinsic to the star. We also show that the Blazhko period is not simply anti-correlated with the long-term period variations as was suggested by previous authors.

Abstrakt: Diskutujeme krátkodobé i dlouhodobé změny pulzační periody Z CVn, klasické hvězdy typu RR Lyrae vykazující Blažkův jev. Z CVn také vykazuje semi-cyklické změny v O-C diagramu, které mohou být interpretovány jako důsledek dvojhvězdnosti v důsledku light travel time efektu. Přinášíme důkaz, že dvojhvězdná hypotéza nemůže být pravdivá a že pozorované dlohodobé změny periody musí být způsobeny jiným mechanismem uvnitř hvězdy. Také ukazujeme, že délka Blažkovy periody není jakkoliv korelována s dlouhodobou změnou periody, jak bylo navrhovanáno v dřívějších pracech.

Introduction

Already a few years after the discovery of the variability of Z CVn (Ceraski 1911), it was realized that the pulsation period monotonically lengthens (Blažko 1922). Firmanyuk (1982) noticed that the pulsation period varies in a cyclic way with period of approximately 80 years and commented that these variations cannot be explained by the binarity, but did not provide any further details. However, if we assume the binary hypothesis, Z CVn would be one of very rare binary candidates with RR Lyrae component.

Short-term cyclic period variations caused by the Blazhko effect with period of 22.75 d were discovered by Kanyó (1966). Le Borgne et al. (2012) suggested that the length of the Blazhko period is anti-correlated with the length of the pulsation period.

In this brief contribution we comment on the anti-correlation of the Blazhko period and period of the long-term period variations, and bring evidences that the long-term pulsation period variations cannot be caused by binarity of Z CVn. All results presented here are based on our research published in Skarka et al. (2018).

Observations, archival data and data analysis

We observed Z CVn photometrically during four seasons in 53 nights and got almost 1200 points in *BVRI* Johnson-Cousins filters using a 20cm telescope (see the phase light curve in Fig. 1). These data have been used for period analysis and estimation of the actual Blazhko period. From the difference between the side peaks and the main pulsation peak shown in the right-hand panel of Fig. 1we got the modulation period 22.931(4) d. We noticed that the pulsation period remains almost constant during the Blazhko effect (variations are bellow 0.01 d) and that the modulation manifests predominantly in brightness (amplitude of about 0.3 mag in *V*).

For the analysis of long-term period evolution we determined 18 maximum times from our data and 51 from various sky surveys (for details see Skarka et al. 2018). We also used archival maximum times provided by the GEOS RR Lyrae database (Le Borgne et al. 2007). Our analysis shows that the long-term variation of the pulsation period is cyclic (as first noticed by Firmanyuk 1982) with period of 78.3 years (left panel of Fig. 2).
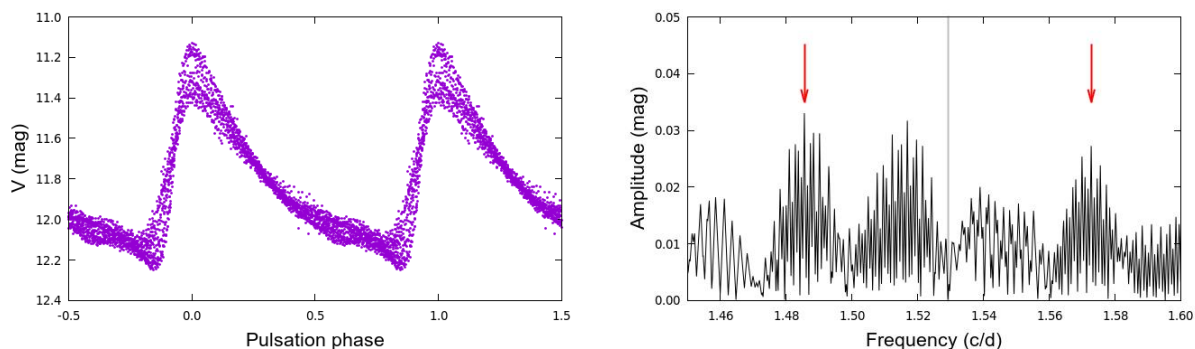
Figure 1: *Left*: Our observations in *V* phased with the pulsation period. *Right*: The frequency spectrum based on our *V* data after prewhitening with the basic pulsation frequency (shown with the grey line) showing the position of the side peaks corresponding to the Blazhko side peaks.
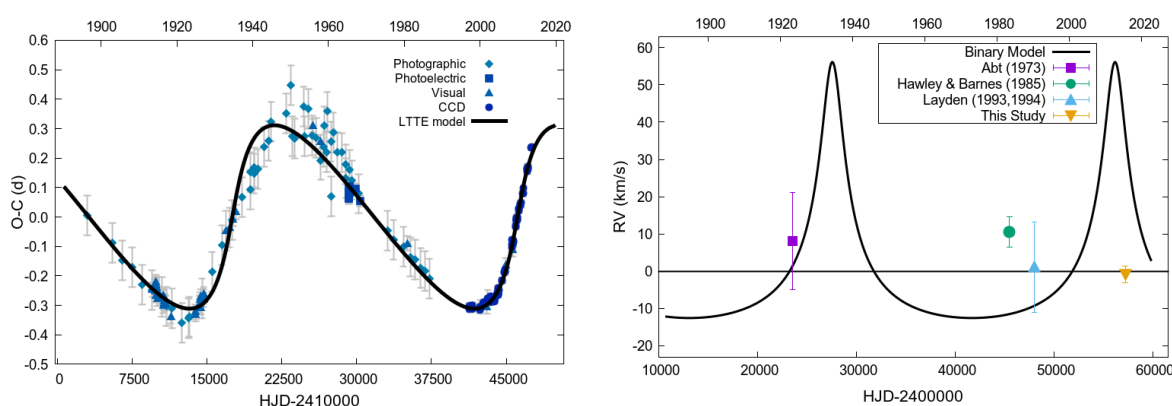

Figure 2: *Left*: Period variations in a form of O-C diagram with the light travel time model (LTTE). *Right*: The radial-velocity model based on the O-C variations (solid line) together with the radial-velocity measurements (points).

We also collected spectroscopic observations with the 2.1m Otto Struve telescope at McDonald observatory, USA (seasons 2015 and 2016). Altogether we determined 11 systemic radial velocities. From the literature we collected additional 8 systemic radial velocities (for details see Skarka et al. 2018).

The length of the Blazhko cycle

Kanyó (1966) determined the Blazhko period as 22.75 d with amplitude 0.033 d. Fourty years later, Le Borgne et al. (2012) estimated the modulation period as 22.98 d with amplitude 0.021 d. This, together with the global evolution of the pulsation period shown in the left panel of Fig. 2, led Le Borgne et al. to the assumption that the length of modulation and pulsation period is anti-correlated.

Our analysis shows Blazhko period of 22.93 d and amplitude of the period variations less than 0.01 d. The pulsation period is similar to the period at the time of Kanyó (1966), but the Blazhko period and amplitude of the period variation during the modulation cycle is different. This shows that there is probably no correlation between the length of modulation and pulsation periods suggested by Le Borgne et al. (2012).

Binary hypothesis

The long-term cyclic period changes can be interpreted as the consequence of binarity and the finite speed of light known as the Light Travel-Time effect. If this hypothesis is true, after modelling the orbit using the O-C, the bottom limit of the mass of an unseen companion is 56.5 Solar masses, which is very unlikely, although not impossible (see the thorough discussion in Skarka et al. 2018). However, the spectroscopic measurements of the

radial velocity disprove the binary hypothesis without a doubt, because measured radial velocities do not match the radial velocity model at all (right-hand panel of Fig. 2).

Discussion and conclusions

On the basis of original measurements and archival data we found that there is probably no correlation between modulation period and the actual value of pulsation period. We also found that cyclic period variations that convincingly resemble the light travel time effect, do not necessarily have to be a consequence of binarity. Thus, majority of binary RR Lyrae candidates must be handled with extreme caution. Our results show that there may be some so far unknown mechanism that is common in RR Lyrae stars and that causes long-term cyclic period variations. Z CVn is a very interesting star that deserves attention because it represents an ideal laboratory for studying period variations and their stability in RR Lyrae stars.

Acknowledgement

References

Abt H. A., 1973, ApJS, 26, 365

Blažko S., 1922, Astron. Nachr., 216, 103

Ceraski W., 1911, Astron. Nachr., 190, 85

Firmanyuk B. N., 1982, Inf. Bull. Var. Stars, 2247

Hawley S. L., Barnes III T. G., 1985, PASP, 97, 551

Kanyó S., 1966, Inf. Bull. Var. Stars, 146

Layden A. C., 1993, PhD thesis, Yale University

Layden A. C., 1994, AJ, 108, 1016

Le Borgne J. F. et al., 2007, A&A, 476, 307

Le Borgne J.-F. et al., 2012, AJ, 144, 39

Skarka, M., Liška, J., Dřevěný, R., et al. 2018, MNRAS, 474, 824